Research Square

Preprints are preliminary reports that have not undergone peer review.
They should not be considered conclusive, used to inform clinical practice,
or referenced by the media as validated information.

What a radical-pair quantum reservoir would require: readable capacity, no quantum advantage, and a nuclear-register criterion

Hikaru Wakaura

hikaruwakaura@gmail.com

QuantScape Inc

Taiki Tanimae

QIRI (Quantum Integrated Research Institute Inc.)

Research Article

Keywords: cryptochrome, quantum reservoir, coherence, quantum-brain

Posted Date: October 30th, 2026

DOI: https://doi.org/10.21203/rs.3.rs-9975866/v2

License: This work is licensed under a Creative Commons Attribution 4.0 International License.
Read Full License

Additional Declarations: The authors declare no competing interests.

What a radical-pair quantum reservoir would require: readable capacity, no quantum advantage, and a nuclear-register criterion

Hikaru Wakaura[1] and Taiki Tanimae[1]

[1] *QIRI (Quantum Integrated Research Institute Inc.), 1–16–3, Akasaka, Minato-ku, Tokyo 107–0061, Japan.*
Correspondence: h.wakaura@qiri.co.jp (ORCID 0000-0001-8381-8323), t.tanimae@qiri.co.jp

(Dated: August 7, 2026)

Whether the electron–nuclear spin coherence behind radical-pair magnetoreception could also support biological *computation* has been conjectured for decades but never made quantitative. We treat a cryptochrome-type radical pair as a reservoir computer, solving the radical-pair master equation with electronic decoherence and driving it as a real turnover does—by the birth of a spin-correlated pair whose singlet character encodes the input. Three results follow, none of them the expected one. The reservoir is *readable by ordinary chemistry*: the nuclear polarisation the product carries away gives an out-of-sample information-processing capacity of 4.7 against its own memoryless floor of 2.0, with no spectroscopy. There is no quantum advantage: a classical network matched channel-for-channel exceeds the five-spin reservoir by 49–123%. And the memory horizon is set not by the microsecond pair lifetime but by the turnover interval, because the nuclear register survives recombination in the diamagnetic product—so the binding constraint is chemical rather than temporal, namely that the *same* register be reused between turnovers. Predicting the register's relaxation instead of assuming it makes that constraint testable: at the geomagnetic field a proton on the intact protein relaxes in milliseconds, not seconds, capping the horizon below the neural band unless the register's dipolar vector reorients about two and a half times faster than the protein ($\tau_{\mathrm{eff}} \lesssim 6$ ns). What survives is a smaller claim on firmer ground: a criterion whose two constants can be measured in vitro, in place of one whose central relaxation time was never measured at all.

I. INTRODUCTION

The radical-pair mechanism (RPM) is the only experimentally established way in which a magnetic field as weak as the geomagnetic field ($\sim 50\ \mu$T) can change the outcome of a chemical reaction [1, 2, 16]. A spin-correlated pair born in a singlet electronic state undergoes coherent singlet–triplet (S–T) interconversion driven by hyperfine fields; because recombination is spin-selective, a field that re-tunes this interconversion alters the product yields. The mechanism underlies the leading model of avian magnetoreception, where the photoreceptor cryptochrome hosts a flavin–tryptophan radical pair [2–5, 12].

The success of the RPM has repeatedly motivated a bolder conjecture: that spin coherence in biomolecules might support not merely sensing but *information processing*—a "quantum brain" [6, 7], a proposal long contested on decoherence grounds [9] and part of the broader programme of quantum biology [10, 11]. A concrete, named instance is the *three-layer quantum-brain hypothesis* [19, 20], which posits a layered architecture—a long-lived nuclear-spin memory (Layer 1), a radical-pair read/write interface (Layer 2), and classical neuronal transduction (Layer 3)—and which, in its most recent form, already reframes the proposal from quantum *computation* to quantum *reservoir dynamics*. The present paper is the quantitative test of that architecture as a reservoir, and the bound it returns. Since that reframing is not new here, we state the delta explicitly: Ref. [20] proposes the reservoir reading and estimates coherence lifetimes, but drives the reservoir by resetting a single electron, reads it through spin observables that presuppose magnetic-resonance access, and identifies the memory horizon with the radical-pair lifetime. What is new here is (i) a chemically consistent drive in which the electron pair is reborn correlated each turnover, (ii) readouts restricted to quantities a downstream reaction could use, each scored against its own memoryless floor, (iii) classical baselines matched by readout dimension, and (iv) the replacement of the lifetime clock by the turnover clock together with the register criterion that follows from it. The spin Hamiltonian, the Haberkorn treatment and the capacity estimators are standard and are not claimed as contributions. A companion study from this program places the conjecture on quantitative footing from the sensing side. Solving the radical-pair master equation with electronic decoherence explicitly included, it finds that the active-site radical pairs of the principal neurotransmitter-metabolising flavoenzymes (monoamine oxidase A/B, D-amino-acid oxidase) are magnetically inert ($< 10^{-4}$% field effect): their large exchange coupling ($|J| \sim 0.75$ GHz) and picosecond lifetimes each independently forbid weak-field S–T mixing. Only a *spatially separated* radical pair, as in cryptochrome—with $J \approx 0$ and a microsecond lifetime—sustains the coherence required for weak-field sensitivity [23, 24]. This premise is a standard result of radical-pair compass theory [2, 23] and is logically independent of the companion analysis; we take the existence of a long-coherence separated radical pair as our self-contained starting point.

This sharp dichotomy invites the question we address here. The separated radical pair is singled out because

it preserves long-lived electron–nuclear spin coherence. *Is that coherence good for anything besides sensing the geomagnetic field?* We argue the question is best posed not as gate-model quantum computation but as *reservoir* computing, and we answer it with the chemistry left in: driven, read and clocked as a turnover actually is. We state at the outset the load-bearing caveat: whether a *neuronal* cryptochrome forms a light- or reaction-driven separated radical pair at all is unestablished—the mammalian CRY1/CRY2 proteins are primarily circadian transcriptional regulators [15]—so every biological conclusion below is conditional on the existence of such a pair. The spin-dynamics results (capacity, classical baselines, the register criterion) do not depend on that condition and stand on their own.

Why a reservoir, not a gate. Gate-model quantum computation treats decoherence as the adversary and demands error correction; a warm, wet, 10^{10}-copy biomolecular ensemble cannot meet that bar. Reservoir computing (RC) inverts the relationship. An RC system feeds a time-dependent input into a fixed nonlinear dynamical "reservoir" and trains only a *linear* readout of its state [25, 26]. RC *requires* dissipation: the echo-state / fading-memory property—that the influence of past inputs decays—is supplied precisely by relaxation [27, 28]. The molecular-spin and NMR communities have demonstrated quantum RC explicitly in nuclear- and electron-spin ensembles [27–29], part of a broad physical-reservoir-computing effort [13]. In this system the fading memory is supplied not by electronic dephasing—varying T_2^e over the physically plausible range 50–2000 ns changes the capacity by under 2%—but by the turnover itself: each cycle discards the electron pair and keeps only the nuclei, which is a dissipative, non-unitary map. It is the openness of the chemical cycle, not the rate of electronic decoherence, that makes the system a reservoir. This is consistent with the large coherence fraction reported below, which is measured in a very different regime: dephasing rates 10^3 times larger than any realistic T_2^e, applied together with a compensating extension of the pair lifetime. Realistic electronic decoherence is not the limiting factor; complete destruction of electronic coherence still is.

Our contribution is to answer that question with the chemistry left in, and the answer overturns three natural expectations. (i) We drive the reservoir as a real turnover does—nuclei retained, a new spin-correlated pair created each cycle—rather than by resetting a single electron, and read it through the products a downstream reaction could actually use. (ii) We compare against classical reservoirs matched by readout dimension, and find no quantum advantage, which we report rather than argue around. (iii) We show that the timescale objection usually raised against this system rests on identifying the reservoir's clock with the radical-pair lifetime, and replace it with a chemical criterion—reuse of the nuclear register—that is falsifiable by chemistry. That criterion still compares two times, as the argument it replaces did; what the spin-dynamical treatment supplies, and no timescale comparison would, is which nuclear relaxation constant appears in it.

The physical correspondence we adopt, adapting the spin-RC framework of Fujii and Nakajima [27], maps the reservoir-computing elements onto the radical pair as follows: the memory nodes are the nuclear spins (in the cryptochrome case ^{14}N and ^{1}H), which store the input in their *populations*, so that the relevant relaxation constant is T_{1n}—though at the geomagnetic field extreme narrowing makes T_{1n} and T_{2n} equal, and both short (Supplemental Material, Sec. S12); the nonlinear read/write head is the radical-pair electron system; the read/write channel is the hyperfine coupling; and the fading memory (echo-state property) is supplied by the openness of the chemical cycle together with inter-cycle nuclear *depolarisation*—not nuclear dephasing, which we show below costs the reservoir almost nothing. These are exactly the three layers of the hypothesis above: Layer 1 (nuclear-spin memory), Layer 2 (the radical-pair interface), and Layer 3 (the classical readout/transduction that trains the linear map).

The paper is organized as follows. Section II establishes the reservoir's capacity and its convergence, localises that capacity in spin coherence, compares it against matched classical baselines, and then asks what a chemical readout recovers; it closes with the reservoir's clock and the nuclear-register criterion. Section III places the result among quantum-brain proposals and states the limitations. The model, protocol, and capacity definitions are collected in Appendix A.

II. RESULTS

We drive the reservoir the way a real turnover does. Each cycle the nuclei are retained and a *new* spin-correlated electron pair is created whose singlet character encodes the input, $\rho_e(s) = s\,|S\rangle\langle S| + (1-s)P_T/3$; the pair then evolves under the Liouville-space master equation with electronic dephasing and, where the readout requires it, spin-selective recombination. This replaces the reset of a single electron used in earlier treatments, which is not a chemical process and which—for a separated pair—destroys the electron–electron correlation every cycle. All capacities are out-of-sample (trained on the first half of a run, scored on the held-out second half). The number of input realisations is not uniform and is stated with each result: 12 for the turnover-clock scan and its paired test, which carry the central claim; 8 for the classical baselines and the T_2^e scan at the engineered point; 6 for the headline capacity, the chemical-readout survey, the route floors, the delay kernel, the grid scans, the nuclide scan and the cryptochrome-point classical baselines; 4 for the register-reuse and nuclear-channel scans and the semiclassical reference; and 3 for the ensemble and anisotropy scans. Four quantities are single-realisation: the ridge and shot-noise sensitivity scans and the semi-

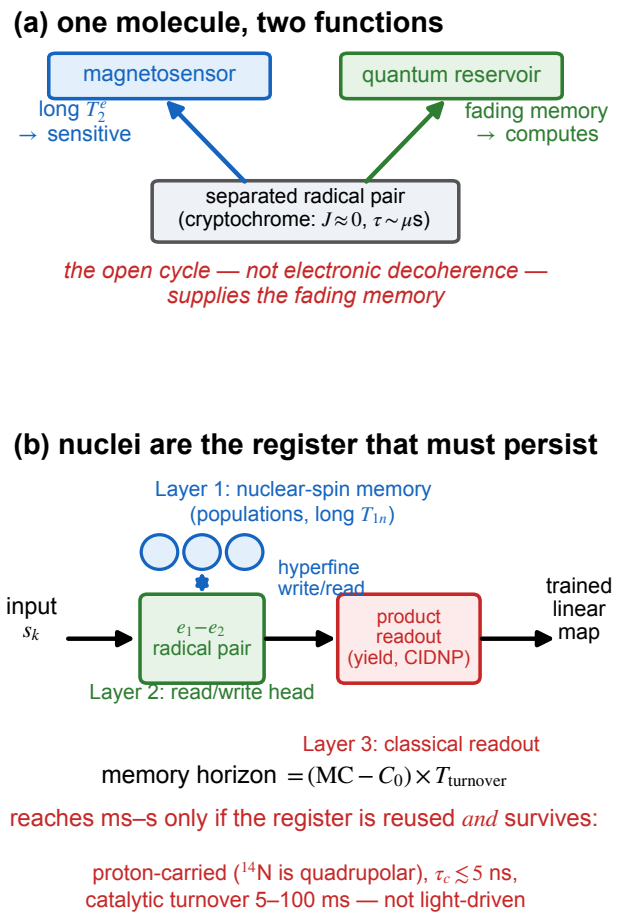


FIG. 1. **The reservoir and the quantity that decides its reach.** (a) A cryptochrome-type separated radical pair ($J \approx 0$, lifetime $\tau \sim \mu$s) is the same molecule in two roles: long electronic coherence makes it a weak-field magnetosensor, while the dissipation of an open cycle supplies the fading memory a reservoir needs. (b) The nuclei are the register: they are not consumed by recombination and therefore persist from one turnover to the next, whereas the electron pair is created afresh each cycle. The memory horizon is consequently set by T_{turnover} and not by τ, and is quoted throughout as $(\mathrm{MC} - C_0) \times T_{\mathrm{turnover}}$, the zero-delay term $C_0 \simeq 1$ carrying no memory. It reaches the neural band only if the register is genuinely reused *and* survives the pause, which requires it to be carried by protons rather than the quadrupolar flavin ^{14}N and to reorient with $\tau_c \lesssim 6$ ns (Supplemental Material, Secs. S9 and S12).

classical integration-step check, which compare variants on one fixed input by design, and the superseded clock scan retained as Supplemental Table S7, whose single realisation is why it was replaced. Model, protocol and estimator are given in Appendix A.

A. Capacity of the reservoir

With a twelve-observable readout the five-spin reservoir attains

$$\mathrm{MC} = 3.9, \qquad \mathrm{IPC} = 5.6 \pm 0.2,$$

of which 1.7 units are nonlinear. Unlike the single-electron-reset protocol, the estimate is converged in the length of the driving sequence: repeating at $L = 600, 1200, 2400, 4800$ gives IPC $= 5.28, 5.60, 5.87, 5.84$, i.e. flat to within the seed-to-seed scatter beyond $L \approx 2400$. The memory kernel decays over ~ 4 cycles, the signature of the fading-memory property.

B. An operational coherence fraction

To ask how much of this is quantum we add a pure-dephasing rate γ in the S_z product basis and take the incoherent limit at *matched hopping rate*: since the golden-rule transfer rate scales as $|H_{ij}|^2/\gamma$, holding rate $\times\, \tau$ fixed requires $\tau \propto \gamma$. Doing so, the capacity saturates at IPC $= 1.00$ for $\gamma = 10^3, 5 \times 10^3, 2 \times 10^4$ MHz — exactly the memoryless floor, i.e. instantaneous read-back of the input with no memory at all. Against the coherent value 5.42 this is a coherence fraction

$$\frac{\mathrm{IPC}_{\gamma=0} - \mathrm{IPC}_{\mathrm{incoh}}}{\mathrm{IPC}_{\gamma=0}} = 0.82. \tag{1}$$

Taking the limit at fixed τ instead, as is sometimes done, measures Zeno freezing rather than the classical limit and inflates this number; we avoid that.

Two caveats are load-bearing. First, γ as applied above acts on all five spins, so one might suspect the collapse merely reflects erasure of the nuclear register rather than loss of electronic coherence. It does not: restricting the added dephasing to the two electrons and leaving the nuclei untouched gives IPC $= 0.9949$, 0.9891 and 0.9891 at the same three rates, i.e. a coherence fraction of 0.817 against 0.816 for the all-spin channel (Supplemental Material, Sec. S5). The number is a statement about the electrons. Second, and more limiting, this is an *operational* fraction defined by one particular matched-hopping construction in which τ is stretched by up to a factor of 400; it is not a decomposition against a physically motivated classical model. The appropriate such reference is a semiclassical radical-pair treatment with classical hyperfine vectors and rate equations [16]. We have since run it (Supplemental Material, Sec. S8): a fully classical model of the same spin system scores at its own memoryless floor, giving a coherence fraction of 0.859, so the 0.82 reported here is if anything conservative. We nonetheless report 0.82 as what it is—the capacity lost under a specific incoherent limit—rather than as a measure of "how quantum" the reservoir is. Note also that this quantity, like the capacity above it, is evaluated at the engineered operating point.

C. There is no quantum advantage

A capacity is only meaningful against a classical reference, and the comparison must be symmetric in what is read out. Driving tanh echo-state networks (ESNs) with the same input and scoring them with the *same* estimator:

TABLE I. The quantum reservoir against matched classical reservoirs at the engineered operating point.

reservoir (readout features)	IPC
quantum, 5 spins (12 observables)	5.59 ± 0.19
ESN, 5 nodes (5 linear features)	4.55 ± 0.32
ESN, 5 nodes (5 linear $+7$ quadratic)	9.41 ± 0.86
ESN, 12 nodes (12 linear features)	10.37 ± 0.59

Matched by *physical unit* the quantum reservoir is modestly ahead (5.59 vs 4.55), but matched by *readout dimension*—the resource that actually sets the Dambre ceiling—a classical system of the same size is well ahead (9.41 vs 5.59). We therefore make no claim of quantum advantage. Which accounting is the fair one depends on a cost model for non-commuting measurements versus multiplications that we do not have; we report the numbers and leave the claim unmade.

That comparison is made at the engineered operating point, which is not the biologically relevant one. Repeating it at the cryptochrome point, against ESNs matched channel-for-channel to the chemical readouts of the next section, removes the ambiguity entirely:

TABLE II. The same comparison at the cryptochrome operating point, matched channel-for-channel.

system (readout features)	IPC
quantum, time-resolved kinetics (5 ch)	2.01 ± 0.09
ESN, 5 nodes (5 features)	4.47 ± 0.33
quantum, kinetics + CIDNP (8 ch)	4.65 ± 0.15
ESN, 8 nodes (8 features)	6.94 ± 0.56
ESN, 12 nodes (12 features)	9.62 ± 0.93

At the cryptochrome point the classical reservoir wins decisively whenever the comparison is matched channel-for-channel: by 49% at eight channels and 123% at five. Matched by *physical unit* instead—five spins against five nodes—the quantum reservoir is nominally ahead, 4.65 ± 0.15 against 4.47 ± 0.33, but that 4% margin is 0.5σ of the seed scatter and we do not read it as an advantage. The honest summary is that the two channel-matched accountings favour the classical system by a wide margin and the third distinguishes nothing. On no accounting does the radical pair compute *better* than a small classical network by a margin exceeding its own seed scatter. That is the honest state of the comparison, and it removes the hedge we left in the preceding paragraph.

D. Biology can read the reservoir

Biology has no EPR spectrometer; it has products. We therefore restrict the readout to observables a downstream reaction could plausibly use, with recombination switched on so that the quantity read is the yield actually produced, $Y_X = k_X \int_0^\tau \mathrm{Tr}[P_X \rho(t)]\, dt$ (Fig. 2):

The memoryless floor is *not* common to these routes, and quoting a single floor of IPC = 1 overstates what the richer readouts achieve. We therefore measure each route's own floor by wiping the nuclear register every cycle ($q = 1$), which leaves only what the route can compute from the present input, and report the excess above it. All seven routes defined by the model are listed; none is omitted.

Four things follow, and only the first is the one we originally reported. First, the readout is genuinely not the limiting resource: time-resolved product kinetics clear their own floor by a factor of two, and the nuclear polarisation the product carries away reaches 4.65 against a floor of 2.01—an excess of 2.64, not the factor of 4.6 that a universal floor of 1 would suggest. The CIDNP route is still the best readout by a wide margin, and it still requires no spectroscopic access.

Second, a single scalar end-point yield gives IPC = 1.02 against a floor of 1.02: it reports the present input and remembers *nothing*. Claims about reservoir behaviour should not be based on it.

Third, the readout saturates in channel count. Doubling the time-resolved kinetics from 5 to 10 channels by adding the second exit channel buys 0.003 in capacity. Whatever limits this reservoir, it is not the number of product observables a downstream reaction can distinguish.

Fourth—and this is a caution about the accumulated-pool route rather than a result—a downstream integrator carries memory of its own. Its floor is 1.96 with a linear memory capacity of 1.94 even when the nuclear register is wiped every single cycle, because the leaky accumulator is itself a classical delay line. Its apparent capacity is therefore not evidence of nuclear-spin memory, and we exclude it from the claims below.

The mechanism behind the CIDNP column is worth stating, because it also explains a negative result. The reduced state of *either* electron of a newly born pair is maximally mixed for every input, since both $|S\rangle\langle S|$ and $P_T/3$ have zero one-electron polarisation; the input lives entirely in the two-electron correlation. With $J = 0$ the two radicals do not interact, so nothing can transfer that correlation to a nucleus—and indeed, with recombination switched off, the cryptochrome-point capacity is 1.01, the memoryless floor. It is *spin-selective recombination* that converts the singlet–triplet correlation into a population difference and so writes the input into the nuclear register. In a separated radical pair, recombination is not merely how the reservoir is read; it is how it is written.

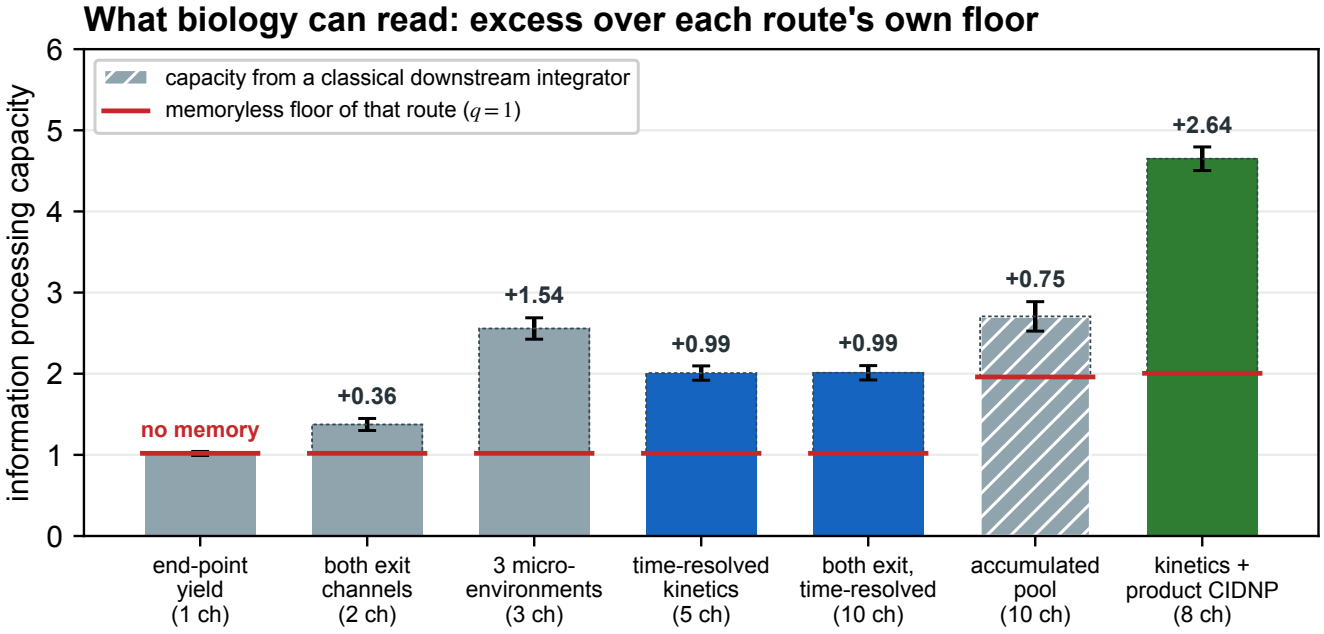


FIG. 2. **Readout is not the bottleneck.** Capacity recovered by chemically accessible observables at the cryptochrome operating point ($B = 50$ μT, $J = 0$, $\tau = 1$ μs), with spin-selective recombination switched on so that the observable is the product actually formed. All seven routes defined by the model are shown. Red bars mark each route's *own* memoryless floor, measured by wiping the nuclear register every cycle ($q = 1$); these are not common to the routes (1.02 for the yield routes, 2.01 for the eight-channel CIDNP route, 1.96 for the accumulated pool), so it is the dashed excess above each floor—printed above each bar—that measures memory, not the bar height. Ordinary reaction kinetics clear their floor by 0.99, and the nuclear polarisation carried away by the product (CIDNP) clears its own by 2.64, the largest of any route. The end-point yield sits exactly on its floor: it reports the present input and remembers nothing. The accumulated pool is hatched because a leaky downstream integrator is itself a classical delay line, so its excess is not evidence of nuclear-spin memory. No spectroscopy is involved.

TABLE III. Capacity recovered by chemically accessible observables at the cryptochrome point, each scored against its own memoryless floor.

readout route	ch.	IPC	floor	excess
end-point singlet yield	1	1.02	1.02	0.00
both exit channels, end point	2	1.37	1.02	0.36
three micro-environments (different τ)	3	2.56	1.02	1.54
time-resolved kinetics, one product pool	5	2.01	1.02	0.99
both exit channels, time-resolved	10	2.01	1.02	0.99
kinetics + CIDNP on the product	8	**4.65**	2.01	**2.64**
kinetics + accumulated downstream pool	10	2.71	1.96	0.75

E. The clock is the turnover, not the pair lifetime

The horizon over which a reservoir remembers is MC multiplied by its cycle time. It is natural, and it is what the submitted version of this work did, to identify that cycle time with the radical-pair lifetime $\tau \sim 1$ μs and conclude that a 3 μs horizon puts the system 10^3–10^5 below neural timescales. That identification is wrong, and its own model says so. The carrier of the memory is the nuclear register, and nuclei are not consumed by recombination: they leave in the diamagnetic product, where nuclear relaxation times are of order 0.1–1 s—a *high-field* figure, which Sec. II F and the Supplemental Material, Sec. S12, revise sharply downwards for the geomagnetic field. The cycle time of the reservoir is therefore the interval between turnovers.

Inserting a pause T_d between turnovers and relaxing the register with probability $q = 1 - \exp(-T_\mathrm{d}/T_{1n})$ (with $T_{1n} = 1$ s) gives Fig. 3(a):

Before the numbers, the horizon needs a definition that is actually a time. MC is a sum of squared correlations over delays $d \geq 0$, and the $d = 0$ term—which reports

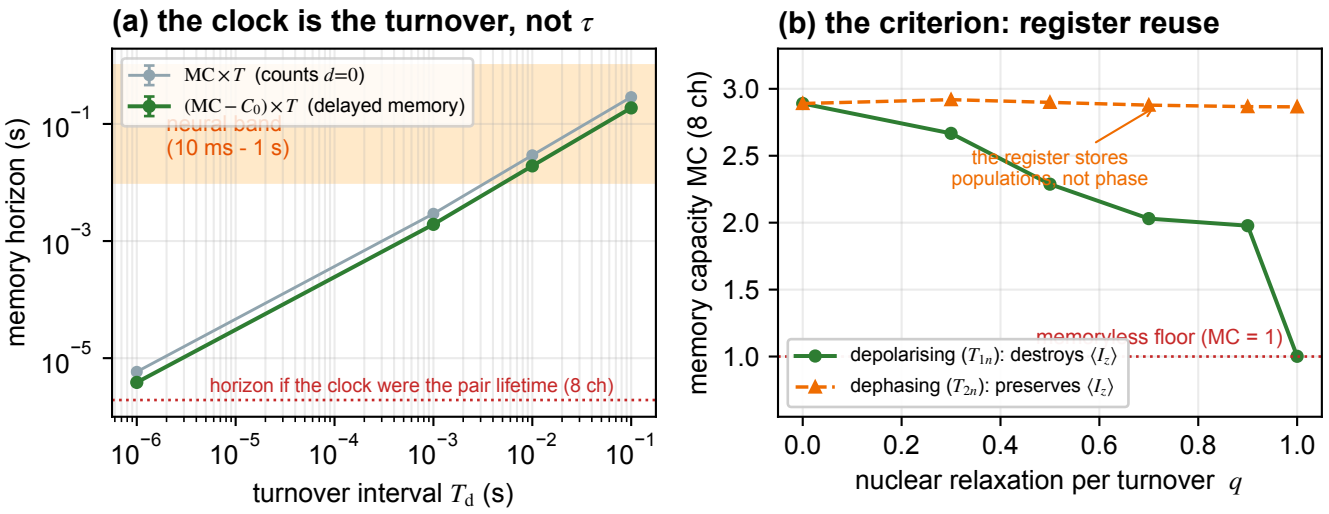


FIG. 3. **(a)** The memory horizon against the turnover interval, from twelve input realisations (error bars are the between-seed standard deviation). Because the nuclear register survives recombination, inserting a physiological pause costs only 1.6% of the memory capacity across five decades, so the horizon simply tracks the clock and enters the neural band (shaded, 10 ms–1 s, the range of cortical rhythms[8]). Both definitions are shown: the raw MC $\times\, T_{\mathrm{turnover}}$ (grey) counts the zero-delay term, which carries no memory, while the delayed-memory horizon $(\mathrm{MC} - C_0) \times T_{\mathrm{turnover}}$ (green) is the quantity quoted in the text—on the latter the 1 ms turnover falls below the band. The dotted line is where the horizon would sit if the clock were the radical-pair lifetime, for the same eight-channel readout. **(b)** The criterion, and which relaxation process enforces it. Depolarising the register between turnovers with probability q (green) drives the capacity to the memoryless floor: at $q = 1$—a fresh molecule each cycle—MC = 1.00 and there is no memory. Pure nuclear *dephasing* at the same q (orange) leaves MC = 2.87, essentially untouched: the register stores populations, not phase, so the constant that bounds the horizon is T_{1n}. Note that this does not lengthen the horizon at the operating point, where extreme narrowing brings T_{1n} and T_{2n} together (Supplemental Material, Sec. S12).

the present input and remembers nothing—contributes $C[0] \simeq 1$ for every readout. Multiplying the raw MC by the cycle time therefore assigns a positive "horizon" to a system with no memory at all, growing without bound as the cycle is lengthened. We instead quote $(\mathrm{MC} - C[0]) \times T_{\mathrm{cycle}}$, the delayed memory only. The measured kernel justifies this: for the CIDNP readout $C[0] = 1.00$, $C[1] = 0.98$, $C[2] = 0.47$, falling below 5% of $C[0]$ by $d = 5$, so $\mathrm{MC} - C[0] = 1.87$ of genuinely delayed capacity.

TABLE IV. The memory horizon against the turnover interval, twelve input realisations.

T_{d}	q	MC (8 ch)	MC × T	$(\mathrm{MC} - C_0) \times T$
1 μs	10^{-6}	2.926 ± 0.149	5.9 μs	3.9 μs
1 ms	10^{-3}	2.926 ± 0.148	2.9 ms	1.9 ms
10 ms	10^{-2}	2.922 ± 0.145	29 ms	19 ms
100 ms	9.5×10^{-2}	2.880 ± 0.116	288 ms	188 ms

Twelve input realisations; the quoted spread is the between-seed standard deviation. Because the same seeds are used at every T_{d}, the change is properly assessed on paired differences: across five decades of turnover interval the capacity falls by 0.046 ± 0.011 (SEM, $n = 12$, $t = 4.23$), that is by 1.6%. This is a real decrease, resolved well above both the seed noise and the time-grid error (0.17% from $n_t = 96$ to 192). It is also roughly eight times larger than the 0.2% quoted in the originally submitted version, which came from a single input realisation and from the five-channel rather than the eight-channel column. The qualitative conclusion is unchanged and now rests on an adequate sample: the capacity is nearly, but not exactly, independent of the turnover interval, so the horizon tracks the clock.

A turnover of 10–100 ms therefore places the memory horizon at 19–188 ms, inside the neural band, *provided the register survives the pause*. That proviso is not free, and Sec. S12 shows it is what now binds: at the geomagnetic field a proton on the intact protein relaxes in 2.4 ms, which caps the horizon at 6.1 ms and puts it below the band unless the register reorients about two and a half times faster than the protein. The numbers in this table should therefore be read as what the spin dynamics permit, not as what the chemistry delivers. We note also that a 1 ms turnover gives 1.9 ms, *below* the 10 ms–1 s band drawn in Fig. 3(a); the originally quoted range of "3–280 ms, inside the neural band" overstated this at its lower end. The timescale objection based on the microsecond pair lifetime does not survive in any of these cases: the same spin physics runs on a slow clock.

F. The criterion: reuse of the nuclear register

What replaces it is a chemical requirement, and a sharper one. Everything above assumes that the register the reservoir writes into is the *same* register on the next turnover. Relaxing that assumption by depolarising the nuclei with probability q between cycles gives Fig. 3(b): the eight-channel memory capacity falls from 2.89 at $q = 0$ to 2.67 at $q = 0.3$ and 2.29 at $q = 0.5$—a loss of a fifth by the time the turnover interval reaches the nuclear relaxation time, not the near-invariance we previously described—then through 2.03 at $q = 0.7$ and 1.98 at $q = 0.9$, and at $q = 1$, a fresh molecule every cycle, collapses to MC = 1.00, the memoryless floor.

Which nuclear relaxation process enforces this can be asked directly. The register we propagate is a full nuclear density matrix, so one might expect memory to require the survival of nuclear coherences as well as populations, making the binding constant $\min(T_{1n}, T_{2n})$. It does not. Replacing the depolarising channel by a pure-dephasing channel on each nucleus, which destroys nuclear coherence while preserving $\langle I_z \rangle$ exactly, leaves the capacity untouched: MC = 2.89 at $q = 0$ and 2.87 at $q = 1$, against 1.00 for the depolarising channel at $q = 1$.

TABLE V. Which nuclear relaxation process enforces the criterion.

q	MC (8 ch), depolarising	MC (8 ch), dephasing
0.0	2.890	2.890
0.5	2.288	2.899
0.9	1.977	2.867
1.0	1.002	2.865

The memory is carried entirely by nuclear z-populations—which is exactly what the CIDNP readout reports—and is indifferent to nuclear phase. The relevant constant is therefore T_{1n} and not T_{2n}.

We must immediately withdraw the rescue this appears to offer. At the geomagnetic field the register is in extreme narrowing ($\omega\tau_c \approx 2 \times 10^{-4}$), and there $J(0)$, $J(\omega)$ and $J(2\omega)$ coincide, so T_{1n} and T_{2n} agree to one part in 10^7 (Supplemental Material, Sec. S12). The distinction between a population register and a coherence register is therefore real as a statement about what the reservoir uses, but it buys nothing at the operating point: both constants take the same, short, value there. It would matter only at fields where $\omega\tau_c \gg 1$, that is, in an NMR magnet rather than in an organism.

It does not, however, make every nucleus eligible. A T_{1n} of order a second is measured for protons in proteins[35]—at high field, the caveat of the preceding paragraph—but ^{14}N is quadrupolar, and at the measured flavin quadrupole couplings and a protein rotational correlation time it relaxes in $\sim$ 0.1–1 μs—faster than any plausible turnover. Two of the three nuclei in our model are the flavin ^{14}N, and they are therefore wiped every cycle whatever the turnover rate. Restricting the register to the tryptophan proton leaves IPC = 2.78 against a floor of 2.01, an excess of 0.78 where the full register gave 2.64; the time-resolved kinetic readout, which needs all three nuclei, falls exactly to its floor (Supplemental Material, Sec. S9). The criterion survives on a proton register, at 29% of the capacity and through the CIDNP channel alone. We regard this as the single most important correction in the present version, because it replaces an assumed relaxation time with a measured one at the cost of most of the capacity.

This is the constraint that actually decides whether a radical pair can serve as a biological reservoir:

> *The same nuclear register must be re-used across successive turnovers, and successive turnovers must be driven by distinct input samples. The register must be carried by protons—the flavin ^{14}N is quadrupolar and cannot hold one—and must reorient with $\tau_c \lesssim$ 6 ns, since at the geomagnetic field a proton whose dipolar vector reorients only with the protein relaxes in* 2.4 *ms on the intramolecular term alone,* 1.6 *ms with the intermolecular bath. Given all of that, the memory horizon is* $(\mathrm{MC} - C_0) \times T_{\mathrm{turnover}}$*, bounded above by* $(\mathrm{MC} - C_0) \times T_{1n}$*; without it, the system retains nothing.*

This criterion is a statement about a spin register. We should be exact about how much of it needed the spin dynamics. The quantity $\mathrm{MC} - C_0 \simeq 1.9$, and with it the horizon, comes from the reservoir calculation. The constants that decide whether the horizon reaches the neural band divide unevenly. The proton T_1 of 2.4 ms and the photon budget are relaxation theory and photophysics and would have followed without the master equation. The 6.1 ms cap and the $\tau_c \lesssim 6$ ns requirement would not: both are obtained by feeding $q = 1 - \exp(-T_\mathrm{d}/T_{1n})$ into the measured MC(q) curve, which is itself an output of the master equation. We previously claimed all four were independent of the spin dynamics; that was wrong for the last two. The population-versus-coherence finding is real, but at the operating point it changes none of those numbers. We therefore claim the spin dynamics for the capacity, not for the criterion's parameters. We should not, however, overstate the distinction we originally drew. Once q is parameterised as $q = 1 - \exp(-T_\mathrm{d}/T_{1n})$, the criterion's quantitative content is a comparison of two times, T_{turnover} against T_{1n}, just as the argument it replaces compared T_{turnover} against τ. What changes is not the form of the argument but which constant appears in it, and that constant is the longer one—by about 2×10^3 for a protein-bound proton at the geomagnetic field, and by $\sim 4 \times 10^5$ for a register that reorients with $\tau_c = 0.1$ ns. The genuinely non-temporal content is the binary chemical requirement that the pair be regenerated on the same molecule.

It is falsifiable by chemistry: it fails if the radical pair is regenerated on a fresh molecule each turnover, or if T_{1n} in the diamagnetic intermediate is faster than the turnover rate. We note that neither T_{turnover} nor T_{1n} has been measured in vivo for a neuronal cryptochrome, so as applied to neurons this is a conditional whose antecedents are not yet accessible. The in vitro route below is proposed because it makes both of them controllable.

G. The register is the product, and that helps

The results above propagate to the next turnover the nuclear state of the pair that did *not* recombine, renormalised. That is a defensible reservoir, but it is not the object the argument of this paper is about: our claim is that the register leaves in the diamagnetic product. The two are disjoint sub-populations of each turnover. We therefore reimplemented the cycle so that the state handed forward is the nuclear density matrix actually carried away by the recombined molecule,

$$\sigma_{\mathrm{nuc}} \propto \int_0^{\tau} \left[k_S \,\mathrm{Tr}_e(P_S \rho P_S) + k_T \,\mathrm{Tr}_e(P_T \rho P_T)\right] \mathrm{d}t, \quad (2)$$

with the electron pair reborn unpolarised, and recomputed every readout route.

TABLE VI. Capacity with the survivor register against the physically faithful product register.

readout route	ch.	survivor	product
end-point singlet yield	1	1.02	1.01
time-resolved kinetics	5	2.01	**2.74**
both exit channels, time-resolved	10	2.01	2.76
kinetics + CIDNP on the product	8	4.65	**4.91**

The chemically correct register is the better one. Time-resolved kinetics rise from 2.01 to 2.74 and the CIDNP route from 4.65 to 4.91; the linear memory capacity rises correspondingly, from 1.97 to 2.44 and from 2.87 to 3.12. The conclusions of this paper are therefore conservative as originally computed. We report the survivor-register numbers throughout because they are the ones the released code produced, and give Eq. (2) as the physically faithful variant. Every result that *reduces* the paper's claims—the proton-only register, the collapse of the kinetic readout under turnover jitter, and the anisotropy cost—has been re-run with the product register and survives (Supplemental Material, Sec. S4). The one quantitative difference is that the kinetic readout degrades more gracefully under half a cycle of jitter with the product register, retaining 18% of its excess at half a cycle where the survivor register retains under 1%; it reaches zero near one and a half cycles. No conclusion in this work depends on the choice.

H. What the numbers depend on

Three sensitivities deserve to be stated, because two of them were not.

Discretisation and sampling. The linear memory capacity—the quantity the turnover-clock claim is about—converges in the time grid: MC = 2.889, 2.866, 2.861 for $n_t = 48$, 96, 192, a change of 0.17% across the last refinement, against the 1.6% effect being claimed. The five-channel capacity is less well converged (1.96, 1.97, 1.95) and we do not base claims on its third digit. The originally submitted turnover-clock scan used a single input realisation and quoted four significant figures; that was not supportable, and the scan is repeated here with twelve.

Regularisation. The linear readout is a ridge with $\lambda = 10^{-6}$ on unstandardised features, and this choice is load-bearing: the time-resolved channels are nested partial integrals of one signal, so the Gram matrix is ill-conditioned ($\kappa \approx 10^9$), and the recovered capacity runs from 4.53 at $\lambda = 10^{-12}$ to 1.98 at $\lambda = 10^{-6}$ to 1.00 at $\lambda = 10^{-1}$ for the kinetic route. Standardising the features raises the values substantially (to 4.34 at $\lambda = 10^{-6}$). The reported capacities are thus *conservative* with respect to this choice rather than inflated by it, but they are not choice-independent, and we no longer present them as though they were.

Counting statistics. The physically meaningful regulariser is the noise on a real product pool. Adding Gaussian shot noise of relative size $N^{-1/2}$ to each channel, for a pool of N molecules, leaves the CIDNP capacity at 4.54 for $N = 10^{10}$ and 4.54 for $N = 10^8$, falling to 3.93 only at $N = 10^6$. At the copy numbers relevant to a cell the readout is not shot-noise limited. This does not address the distinct question of whether 10^{10} copies driven by a common input but not phase-locked to a common turnover schedule retain the single-molecule capacity after pooling; that is computed in Sec. S10 and reported under Limitations below, where it turns out to be the more severe of the two effects.

III. DISCUSSION

What changed, and why it matters. Three claims that are natural to make about this system—that a scalar chemical readout is too impoverished to be useful, that a spin reservoir of a few spins beats a classical system of the same size, and that microsecond radical-pair lifetimes put biological computation out of reach—all fail when the model is driven as a real turnover and compared symmetrically. The readout is not the bottleneck; the quantum advantage is not there, and at the biologically relevant operating point no accounting we can construct puts the radical pair ahead by more than its own seed scatter; and the timescale gap is an artifact of identifying the reservoir clock with the pair lifetime rather than the turnover interval. What remains is a chemical criterion, together

with the structural fact that the register stores populations rather than coherence and is therefore governed by T_{1n}. That fact does not, however, rescue the biological reading as we first supposed: at the geomagnetic field extreme narrowing makes T_{1n} and T_{2n} equal, and both short, so what the criterion now demands is a register that reorients fast enough to lengthen them.

Relation to prior work. Quantum reservoir computing in spin ensembles is established, including the use of dissipation as a resource and the exponential-state-space argument.[13, 27–30] We do not claim these as new, and—having found no advantage under a symmetric comparison—we do not add to them. The question of whether nuclear polarisation accumulates usefully across successive cryptochrome photocycles has been asked before, by Wong *et al.*[36], who found that the gain available in an idealised model does not survive conditions approaching those in vivo. Our criterion is the chemical statement of what would have to be true for it to survive, and our conclusions are consistent with theirs: the reservoir works only in a narrow and specific corner of parameter space. Photo-CIDNP itself has been observed in a flavoprotein[41] though not yet in cryptochrome, and the underlying polarisation mechanism is standard[18]. Our contribution is to take a chemically realised radical pair, drive and read it as chemistry actually would, and convert a long-standing qualitative conjecture[6, 7] into a criterion that experiment can test. The decoherence objection usually cited against such proposals[9] does not apply directly here: it evaluates superpositions of ion positions and tubulin dipole states, not nuclear spins, which is precisely why nuclear-spin proposals were advanced in reply to it. The objection that does apply is the one this work inherits—nuclear relaxation in the diamagnetic product—and the relevant history is discouraging. The long ^{31}P coherence times underpinning Ref. [6] are theoretical estimates rather than measurements, and have since been bounded at 37 min and expected at "a few seconds" by spin-dynamics calculation[37], while ^{31}P singlet order in pyrophosphate is measured to relax *faster* than T_1[34]. We therefore ground our own relaxation assumption on measured proton T_1 values in proteins rather than on estimate, and restrict the register accordingly (Supplemental Material, Sec. S9). The result also sharpens why CIDNP matters here: in a separated pair it is not an optional extra channel but the mechanism by which information reaches the nuclei at all.

Limitations. The model is a five-spin reduction. Two of its simplifications have now been relaxed, with opposite outcomes. Treating ^{14}N correctly as spin-1 rather than spin-1/2 *increases* the excess capacity by 28%, so that approximation was conservative. Anisotropy is not: scanning an axial hyperfine tensor at fixed isotropic average costs roughly two-thirds of the capacity by $\eta = 0.5$, and the capacity vanishes exactly at the Ising point where the perpendicular components go to zero, which identifies those components as what carries the memory (Supplemental Material, Sec. S11). That scan is not a calculation with the published tensor sets of the cryptochrome pair[21, 22], which we still do not treat, so the limitation is narrowed rather than removed—but the direction is unfavourable and we report it as such. The capacity estimator uses degree-2 targets, so higher-order nonlinear capacity is not counted. Whether a *neuronal* cryptochrome forms a separated radical pair at all is unestablished—CRY1/CRY2 are primarily circadian transcriptional regulators[15]—so the biological reading of our criterion is conditional. The spin-dynamics results do not depend on that condition.

Four further conditions bound the biological reading. Three we have now quantified, and each cost the paper something.

(i) *Which nuclei hold the register.* Not all of them. Nuclear *dephasing* turns out to be irrelevant—the register is a population register—so the binding constant is T_{1n} as assumed. But T_{1n} is not one number. Protein-bound ^{1}H relaxes on the second timescale in the measurements available[35]—all of them at NMR field strengths, a caveat item (iv) below makes decisive—whereas ^{14}N is quadrupolar and, at the measured flavin quadrupole couplings and a protein correlation time, relaxes in ~ 0.2–0.3 μs at the geomagnetic field and in single microseconds even at 9.4 T[38, 39]—faster than any physiological turnover at either. Two of our three nuclei are ^{14}N, and they cannot hold a register at any physiological turnover rate. Restricting the register to the proton leaves 29% of the excess capacity and destroys the time-resolved kinetic readout entirely. Of the two routes we tested under this restriction, CIDNP is the one that survives; the other five routes were not re-evaluated with a restricted register (Supplemental Material, Sec. S9). The turnover-clock argument survives, on measured rather than assumed relaxation data; the capacity does not survive intact.

(ii) *Ensemble averaging.* Pooling $\sim 10^{10}$ copies is safe against heterogeneity—of the couplings and, separately, of the relaxation rate—but not against desynchronisation. Letting τ_c vary log-normally over a sixteen-fold range, so that copies retain different fractions of their register, leaves the CIDNP excess at 2.04 against 1.96 for a uniform pool: capacity does not fall, and the whole effect is under five per cent. A mean-field control at the pool's own mean survival accounts for only a third of even that small difference, so a heterogeneous pool is not simply a homogeneous one at its mean T_{1n}; a single effective T_{1n} is a working approximation rather than an identity (Supplemental Material, Sec. S10). The kinetic readout's memory falls away with the spread of copy phases: with the product register its excess declines from 1.72 at zero jitter to 0.32 at half a cycle, 0.18 at one cycle and 0.02 at one and a half, and with the survivor register it is already at 0.01 by half a cycle. Two cautions attach to reading those numbers as a smooth decay. The survivor sequence is not monotonic—it returns to 0.11 at one cycle—and the register-wiped floor itself rises steeply beyond one cycle (from 1.01 to 1.86 for the product register), because pooling copies that sit whole cycles apart

is itself a delay line. The excess is the right quantity precisely because it subtracts that, but the underlying capacities do not fall monotonically and we do not claim they do. CIDNP retains 40–49% of its excess even at two cycles of jitter, depending on the register, because it integrates over the cycle rather than sampling it (Sec. S10). Synchronised turnover is thus a requirement of the kinetic readout specifically. Both restrictions—nuclide and desynchronisation—leave CIDNP as the surviving one of the two routes tested under each.

(iii) *Readout signal-to-noise.* The ridge parameter is an implicit noise model and the recovered capacity depends on it (Sec. II H); the reported values are conservative with respect to that choice, and adding Poisson shot noise for a pool of 10^8 molecules or more leaves them essentially unchanged.

(iv) *Falsifiability.* Neither T_{turnover} nor T_{1n} has been measured for a neuronal cryptochrome, but both can be predicted from measured constants, and doing so sharpens the criterion into something testable without a neuron (Supplemental Material, Sec. S12). Two results follow, and the first is adverse. Nuclear relaxation at the geomagnetic field is in the extreme-narrowing regime, where $1/T_1 \propto \tau_c$ is maximal, so the second-long T_{1n} we assumed is a *high-field* value: a proton on a 60 kDa protein relaxes in 2.4 ms at 50 μT against 9.0 s at 9.4 T. What sets the ceiling is not whether the register is chemically bound to the protein but the effective correlation time of its dipolar vector, $\tau_{\mathrm{eff}} = S^2\tau_c + (1 - S^2)\tau_{\mathrm{int}}$, together with the dipolar sum $\Sigma = \sum_j S_j^2 r_j^{-6}$ over intramolecular *and* intermolecular partners. For a vector that reorients only with the intact 60 kDa protein ($S^2 = 1$, $\tau_c = 15.2$ ns) the intramolecular geminal term alone gives $T_1 \leq 2.4$ ms and a ceiling of ≤ 6.1 ms; adding the intermolecular proton bath—whose size we calibrate on the water row of our own validation table, at 54% of the intramolecular rate—shortens these to 1.6 and 4.0 ms. That row is an empirical anchor rather than an independent check: f is defined as its residual, so the agreement it then shows is an identity. Fast internal motion lengthens T_1: the intramethyl H–H vector of the flavin 8α-CH_3 has the exact geometric value $S^2 = 1/4$, because that vector does *not* co-rotate rigidly with the protein even though the methyl is covalently attached, and the intramethyl coupling alone would give $T_1 = 5.0$ ms and a ceiling of 11.3 ms—inside the band. That escape does not survive the bath: it moves the methyl's own boundary from 19.3 to 10.8 ns. The criterion is therefore quantitative and vector-specific rather than a statement about binding: the register's dipolar vector must lose orientational memory about two and a half times faster than the intact protein ($\tau_{\mathrm{eff}} \lesssim 6$ ns), a factor that would be 1.6 if the intermolecular bath were neglected. Second, the drive cannot be light: with the measured flavin extinction coefficient, a single flavin turns over once per 7.7 s in full sunlight and once per some hundreds of years inside a skull, so a photochemical cycle fails by about ten orders of magnitude and the regeneration must be catalytic. The criterion that survives is correspondingly specific—the pair regenerated catalytically on a register with $\tau_c \lesssim 6$ ns, at a turnover interval that depends on how mobile that register is—9.8–27 ms at $\tau_c = 5$ ns, widening to 5.6–134 ms at 1 ns and 5.4–1340 ms at 0.1 ns—and both of its parameters are measurable in vitro by relaxation dispersion and steady-state kinetics.

What would settle it. The criterion is addressable in vitro before it is addressable in a neuron. Covalently linked donor–bridge–acceptor radical pairs have synthetically tunable exchange coupling and lifetime and are read by transient EPR and optical/CIDNP spectroscopy.[2, 14, 42] Repeatedly cycling such a system and asking whether the product yield of turnover k depends on the input at turnover $k-1$, $k-2$, ... measures the memory horizon directly, and varying the interval between cycles tests the register-reuse criterion where it is sharpest.

IV. CONCLUSION

Driven and read as a chemical turnover rather than as an abstract quantum channel, a cryptochrome-type radical pair is a reservoir whose output ordinary chemistry can recover: time-resolved product kinetics give IPC = 2.0 against a floor of 1.0, and the nuclear polarisation carried off by the product reaches 4.7 against a floor of 2.0, with no spectroscopic access required. Under a specific matched-hopping incoherent limit 82% of that capacity is lost, and the loss is attributable to the electrons rather than to erasure of the nuclear register—and yet there is no quantum advantage: at the biologically relevant operating point a classical network matched channel-for-channel exceeds the radical pair. The obstacle usually invoked, a microsecond memory horizon, does not survive scrutiny: the register is nuclear and survives recombination, so the clock is the turnover interval, and a 10–100 ms turnover places the horizon at 19–188 ms—so long as the register itself lasts that long, which for a vector reorienting only with the whole protein nucleus at the geomagnetic field it does not. What decides the question instead is whether the same nuclear register is reused from one turnover to the next; if it is not, the capacity falls to a memoryless MC = 1. Because that register stores its information in nuclear populations rather than in nuclear coherence, the constant that bounds it is a nuclear T_1. That distinction, which we first took to be what rescued the horizon, in fact buys nothing at the operating point: the geomagnetic field puts the register in extreme narrowing, where T_{1n} and T_{2n} are equal. It cannot, however, be any nucleus. The flavin ^{14}N is quadrupolar and relaxes in microseconds, so the register must be carried by protons; that restriction removes seven tenths of the *excess* capacity—the IPC itself falls by two fifths—and leaves the product's nuclear polarisation as the only readout we tested that still works, a conclusion reached independently by asking what survives when the copies

in a 10^{10}-molecule pool fall out of step. We offer the criterion as the thing to test, in the sharpened form that the relevant constant is the proton T_1 of the diamagnetic product *at the geomagnetic field*, which our own calculation puts at 2.4 ms—1.6 ms once the intermolecular bath is restored—for a nucleus whose dipolar vector reorients only with the protein, rather than at the second suggested by high-field measurements—so that the register must reorient at least two and a half times faster than the protein for the horizon to reach the neural band at all. The turnover interval of a neuronal cryptochrome has not been measured.

ACKNOWLEDGMENTS

We thank the reviewers of the companion sensing study, whose insistence on decoherence-explicit treatment shaped the methodology used here. All numerical results are reproducible from the open-source `qbscreen` package.

AUTHOR CONTRIBUTIONS

H.W. conceived the study, developed the master-equation and reservoir code, ran the simulations, and wrote the manuscript. T.T. contributed to the spin-dynamics formulation and the analysis of the nuclear-register criterion. Both authors reviewed the results and approved the manuscript.

Appendix A: Model and methods

1. Reservoir Hamiltonian

We model the reservoir as $N = 5$ spins—two radical-pair electrons (e_1, e_2) and three spin-1/2 nuclei—with Hamiltonian (in MHz). At the cryptochrome point the three nuclei carry the hyperfine couplings of ^{14}N5 and ^{14}N10 on FAD$^{\bullet-}$ and Hβ1 on TrpH$^{\bullet+}$ (Supplemental Material, Table S19), with ^{14}N modelled as spin-1/2; no ^{31}P is present in the cryptochrome model, and the ^{31}P-based proposal of Ref. [6] is therefore *not* the system tested here.

$$H = \omega_e\,(S_z^{e_1} + S_z^{e_2}) + \sum_{\mu=x,y,z} \Big[A_P\, S_\mu^{e_1} I_\mu^{P} + A_{H_1} S_\mu^{e_1} I_\mu^{H_1} + A_{e_2} S_\mu^{e_2} I_\mu^{H_2} + J\, S_\mu^{e_1} S_\mu^{e_2} \Big], \tag{A1}$$

where $\omega_e = g_e \mu_B B/h$ is the electron Zeeman frequency. Each radical carries its own nuclei—they are not shared, which is what a spatially separated pair means—and the exchange J links the two electrons. At the engineered operating point we use $A_{e_1 a} = 80$, $A_{e_1 b} = 40$, $A_{e_2 a} = 15$ MHz, $J = 2$ MHz and $B = 1$ mT: representative molecular-spin-RC values chosen to give effective hyperfine writing, not a fit to a specific protein. For the cryptochrome point we set $J = 0$, $B = 50$ μT and $\tau = 1$ μs, with hyperfine magnitudes representative of the dominant FAD$^{\bullet-}$ and TrpH$^{\bullet+}$ couplings [21, 22]. The capacity is not fine-tuned to these numbers: it varies by under 2% over $T_2^e = 50$–2000 ns. It does fall steeply *below* the operating point (-47% from 50 to 5 ns), where the pair lifetime becomes decoherence-limited, so the insensitivity claimed here is to T_2^e at or above τ, not to T_2^e generally. The register criterion of Sec. II F, however, is *not* independent of the hyperfine assignment—it is carried by the perpendicular tensor components and vanishes with them (Supplemental Material, Sec. S11).

2. Master equation and propagator

Each reservoir update is the completely positive, trace-preserving map $\rho \mapsto e^{\mathcal{L}\tau}\rho$ generated by the Haberkorn master equation [31] (whose spin-selective recombination operator we adopt in its standard form [17]) with electronic pure dephasing,

$$\frac{d\rho}{dt} = -i[H,\rho] - \tfrac{1}{2}\{k_S P_S + k_T P_T, \rho\} + \sum_i \frac{1}{T_2^e}\big(S_z^i \rho S_z^i - \tfrac{1}{4}\rho\big)\,, \tag{A2}$$

solved exactly in Liouville space. The third term is the electronic decoherence that the companion sensing analysis showed to be decisive; it is not, however, what supplies the fading memory here, which comes from the openness of the chemical cycle and from inter-cycle nuclear depolarisation. We verified that, in the limit $1/T_2^e \to 0$ and $k_S = k_T$, the Liouville-space solver reproduces the closed-form coherent Green's-function singlet yield to better than 10^{-9} (Supplemental Material). Whether recombination acts within the update step depends on which result is being computed; the two conventions are set out under "Reservoir protocol" below.

3. Reservoir protocol

We adapt the temporal-QRC protocol of Ref. [27], but the drive is *not* the single-electron reset used there. At step k the nuclei are retained and the electron pair is recreated as a spin-correlated pair whose singlet character encodes the input,

$$\rho_e(s_k) = s_k\,|S\rangle\langle S| + (1 - s_k)\,P_T/3, \tag{A3}$$

so that the reservoir state entering cycle k is $\rho_e(s_k)\otimes\sigma_{\mathrm{nuc}}^{(k)}$. The state then evolves for the pair lifetime τ under $e^{\mathcal{L}\tau}$; a set of observables is read out, and a linear (ridge) readout is trained on them. Inputs s_k are i.i.d. uniform on $[0,1]$; the first 80–100 steps are discarded as washout. The

washout discards initial transients, so the reported capacities are independent of the initial spin state—a consequence of the fading-memory (echo-state) property.

Two operating points are used and must not be conflated. The *engineered* point ($J = 2$ MHz, $B = 1$ mT, $\tau = T_2^e = 50$ ns) is a molecular-spin-RC reference and is where the twelve-observable capacity, the coherence fraction and the classical baselines of Secs. II are evaluated; it lies outside the weak-field separated-pair regime that motivates the biological reading, and we flag every number taken there. The *cryptochrome* point ($J = 0$, $B = 50\ \mu$T, $\tau = 1\ \mu$s, $T_2^e = 1\ \mu$s) is where the chemically accessible readouts, the turnover clock and the register criterion are evaluated. Recombination is likewise not uniform across the paper: the twelve-observable capacity is computed with $k_S = k_T = 0$ within the update step, whereas every chemical-readout, clock and criterion result is computed with spin-selective recombination acting throughout the cycle ($k_S = 1$, $k_T = 0.2\ \mu\text{s}^{-1}$).

The single-electron reset of Ref. [27], in which only the input electron is replaced by a product state while the reduced state of the remainder is retained, is used in this work *only* as a control. It is not a chemical process, and for a separated pair ($J = 0$) it destroys the electron–electron correlation every cycle: since $\langle P_S\rangle = \frac{1}{4} - \langle \boldsymbol{S}_1 \cdot \boldsymbol{S}_2\rangle$ with $\langle \boldsymbol{S}_2\rangle = 0$, the singlet probability is pinned at exactly 1/4 independently of the input, and the measured capacity is identically zero (Supplemental Material, Sec. S3). All results reported below use Eq. (A3).

4. Capacity measures

We quantify the reservoir with two information-theoretic benchmarks. The linear *memory capacity* [32] $\text{MC} = \sum_{d\geq 0} r^2(s_{k-d})$ sums the squared multiple correlation for reconstructing delayed inputs. The *information processing capacity* [33] adds nonlinear functions of the input history, $\text{IPC} = \text{MC} + \sum_{\text{nonlinear}} C$, evaluated here through degree-2 Legendre targets (diagonal $P_2(s_{k-d})$ and cross $s_{k-d_1}s_{k-d_2}$ terms). A fundamental theorem [33] bounds the total capacity by the number of linearly independent readout observables, $\text{IPC} \leq n_{\text{obs}}$; we use this bound throughout as a correctness anchor. It is an asymptotic bound for an orthonormal target family and is violated by a few per cent in finite samples, so satisfying it does *not* demonstrate that the readout observables are independent, and we make no such argument anywhere (Supplemental Material, Sec. S2).

All results are reproducible from the open `qbscreen` package; the module list is given under Data and code availability below. We note there that `ensemble.py`, `quantum_vs_classical.py` and the `run_reservoir` driver in `reservoir.py` still implement the superseded single-electron reset and are retained only as controls, so no result reported here is taken from them; the capacity estimators in `reservoir.py` are used throughout (286/286 tests pass).

Appendix B: Data and code availability

All analyses are implemented in the open `qbscreen` package, `https://github.com/deeptell-inc/new_Q_brain`. The corrected correlated-pair-birth injection is in `qbscreen/corrected_injection.py`; the chemically accessible readout routes, the turnover-clock scan and the register-reuse criterion are in `qbscreen/readout_routes.py`; the protocol-consistent capacity, coherence fraction and classical baselines are in `qbscreen/final_numbers.py`; the master-equation solver is in `qbscreen/master_equation.py`. Numerical outputs are in `simulation_results/`. The capacity bound and the agreement of the solver with the closed-form coherent limit are checked in `qbscreen/tests/` (286 tests, all passing). Twenty-nine tests in `test_panel_claims.py` bind the headline quantities and load-bearing claims, and a further one hundred and forty in `test_table_rows.py` bind the capacity and standard-deviation cells of every table in the main text and Supplemental Material, with the expected values transcribed from the manuscript rather than from the data files. The opposite direction is checked by `test_printed_cells.py`, which parses the numeric cells back out of the `.tex`: the headline tables are matched column by column against their data files, and every other printed table cell must equal some shipped value. The suite therefore fails if either side moves. The spin-parameter table (S19) is now bound as well, by `test_spin_parameters.py`: it parses the printed values and compares them to the dictionaries the Hamiltonian is built from, checking the millitesla column as the megahertz column divided by the electron gyromagnetic ratio rather than as an independent input. Derived-time and raw-IPC columns remain unbound. Hand-typed cross-document references to supplement tables, which LaTeX cannot check across separate documents, are bound against `supplementary.aux` by `test_cross_document_refs.py`. This closes the drift that produced the error the present revision began with, in which a figure quoted from the five-channel column was printed beside the eight-channel table.

[1] U. E. Steiner and T. Ulrich, *Magnetic field effects in chemical kinetics and related phenomena*, Chem. Rev. **89**, 51 (1989).

[2] P. J. Hore and H. Mouritsen, *The radical-pair mechanism of magnetoreception*, Annu. Rev. Biophys. **45**, 299 (2016).

[3] T. Ritz, S. Adem, and K. Schulten, *A model for photoreceptor-based magnetoreception in birds*, Biophys. J. **78**, 707 (2000).

[4] K. Maeda *et al.*, *Magnetically sensitive light-induced reactions in cryptochrome are consistent with its proposed role as a magnetoreceptor*, Proc. Natl. Acad. Sci. USA **109**, 4774 (2012).

[5] J. Xu *et al.*, *Magnetic sensitivity of cryptochrome 4 from a migratory songbird*, Nature **594**, 535 (2021).

[6] M. P. A. Fisher, *Quantum cognition: The possibility of processing with nuclear spins in the brain*, Ann. Phys. **362**, 593 (2015).

[7] C. M. Kerskens and D. López Pérez, *Experimental indications of non-classical brain functions*, J. Phys. Commun. **6**, 105001 (2022).

[8] G. Buzsáki and A. Draguhn, *Neuronal oscillations in cortical networks*, Science **304**, 1926 (2004).

[9] M. Tegmark, *Importance of quantum decoherence in brain processes*, Phys. Rev. E **61**, 4194 (2000).

[10] N. Lambert, Y.-N. Chen, Y.-C. Cheng, C.-M. Li, G.-Y. Chen, and F. Nori, *Quantum biology*, Nat. Phys. **9**, 10 (2013).

[11] J. Cao *et al.*, *Quantum biology revisited*, Sci. Adv. **6**, eaaz4888 (2020).

[12] H. G. Hiscock *et al.*, *The quantum needle of the avian magnetic compass*, Proc. Natl. Acad. Sci. USA **113**, 4634 (2016).

[13] G. Tanaka *et al.*, *Recent advances in physical reservoir computing: A review*, Neural Netw. **115**, 100 (2019).

[14] M. R. Wasielewski *et al.*, *Exploiting chemistry and molecular systems for quantum information science*, Nat. Rev. Chem. **4**, 490 (2020).

[15] C. L. Partch, C. B. Green, and J. S. Takahashi, *Molecular architecture of the mammalian circadian clock*, Trends Cell Biol. **24**, 90 (2014).

[16] C. R. Timmel, U. Till, B. Brocklehurst, K. A. McLauchlan, and P. J. Hore, *Effects of weak magnetic fields on free radical recombination reactions*, Mol. Phys. **95**, 71 (1998).

[17] J. A. Jones and P. J. Hore, *Spin-selective reactions of radical pairs act as quantum measurements*, Chem. Phys. Lett. **488**, 90 (2010).

[18] P. J. Hore and R. W. Broadhurst, *Photo-CIDNP of biopolymers*, Prog. Nucl. Magn. Reson. Spectrosc. **25**, 345 (1993).

[19] H. Wakaura, *Systematic screening of brain neurotransmitter enzymes for radical-pair mechanism competence identifies candidates for magnetic field sensitivity*, Research Square preprint, doi:10.21203/rs.3.rs-9278975/v1 (2025).

[20] H. Wakaura, *Motional narrowing rescues entanglement in biological radical-pair systems: quantum error correction and reservoir computing beyond the breaking threshold*, Research Square preprint, doi:10.21203/rs.3.rs-9493052/v1 (2026).

[21] A. A. Lee, J. C. S. Lau, H. J. Hogben, T. Biskup, D. R. Kattnig, and P. J. Hore, *Alternative radical pairs for cryptochrome-based magnetoreception*, J. R. Soc. Interface **11**, 20131063 (2014).

[22] E. Schleicher *et al.*, *Selective* ^{13}C *labelling reveals the electronic structure of flavocoenzyme radicals*, Sci. Rep. **11**, 18395 (2021).

[23] O. Efimova and P. J. Hore, *Role of exchange and dipolar interactions in the radical pair model of the avian magnetic compass*, Biophys. J. **94**, 1565 (2008).

[24] H. Wakaura and T. Tanimae, *Electronic decoherence and exchange coupling preclude weak-field magnetosensitivity of neurotransmitter-metabolising flavoenzymes* (companion manuscript, 2026).

[25] W. Maass, T. Natschläger, and H. Markram, *Real-time computing without stable states: A new framework for neural computation based on perturbations*, Neural Comput. **14**, 2531 (2002).

[26] H. Jaeger and H. Haas, *Harnessing nonlinearity: Predicting chaotic systems and saving energy in wireless communication*, Science **304**, 78 (2004).

[27] K. Fujii and K. Nakajima, *Harnessing disordered-ensemble quantum dynamics for machine learning*, Phys. Rev. Applied **8**, 024030 (2017).

[28] K. Nakajima *et al.*, *Boosting computational power through spatial multiplexing in quantum reservoir computing*, Phys. Rev. Applied **11**, 034021 (2019).

[29] R. Martínez-Peña *et al.*, *Dynamical phase transitions in quantum reservoir computing*, Phys. Rev. Lett. **127**, 100502 (2021).

[30] P. Mujal, R. Martínez-Peña, J. Nokkala, J. García-Beni, G. L. Giorgi, M. C. Soriano, and R. Zambrini, *Opportunities in quantum reservoir computing and extreme learning machines*, Adv. Quantum Technol. **4**, 2100027 (2021).

[31] R. Haberkorn, *Density matrix description of spin-selective radical pair reactions*, Mol. Phys. **32**, 1491 (1976).

[32] H. Jaeger, *Short term memory in echo state networks*, GMD Report 152, German National Research Center for Information Technology (2002).

[33] J. Dambre, D. Verstraeten, B. Schrauwen, and S. Massar, *Information processing capacity of dynamical systems*, Sci. Rep. **2**, 514 (2012).

[34] D. E. Korenchan, J. Lu, M. H. Levitt, and A. Jerschow, ^{31}P *nuclear spin singlet lifetimes in a system with switchable magnetic inequivalence: experiment and simulation*, Phys. Chem. Chem. Phys. **23**, 19465 (2021).

[35] N. Tjandra, S. E. Feller, R. W. Pastor, and A. Bax, *Rotational diffusion anisotropy of human ubiquitin from* ^{15}N *NMR relaxation*, J. Am. Chem. Soc. **117**, 12562 (1995).

[36] S. Y. Wong, I. A. Solov'yov, P. J. Hore, and D. R. Kattnig, *Nuclear polarization effects in cryptochrome-based magnetoreception*, J. Chem. Phys. **154**, 035102 (2021).

[37] T. C. Player and P. J. Hore, *Posner qubits: spin dynamics of entangled* $Ca_9(PO_4)_6$ *molecules and their role in neural processing*, J. R. Soc. Interface **15**, 20180494 (2018).

[38] Y. A. Goddard, J.-P. Korb, and R. G. Bryant, *Water molecule contributions to proton spin–lattice relaxation in rotationally immobilized proteins*, J. Magn. Reson. **199**, 68 (2009).

[39] E. P. Sunde and B. Halle, *Mechanism of* ^{1}H–^{14}N *cross-relaxation in immobilized proteins*, J. Magn. Reson. **203**, 257 (2010).

[40] W. Bogner *et al.*, *Assessment of* ^{31}P *relaxation times in the human calf muscle: a comparison between 3 T and 7 T in vivo*, Magn. Reson. Med. **62**, 574 (2009).

[41] S. S. Thamarath, J. Heberle, P. J. Hore, T. Kottke, and J. Matysik, *Solid-state photo-CIDNP effect observed in phototropin LOV1-C57S by* ^{13}C *magic-angle spinning NMR spectroscopy*, J. Am. Chem. Soc. **132**, 15542 (2010).

[42] M. R. Wasielewski, *Energy, charge, and spin transport in molecules and self-assembled nanostructures inspired by photosynthesis*, J. Org. Chem. **71**, 5051 (2006).